Journal Pre-proof

Electrothermal responsive self-healing for carbon fiber/epoxy interphase based on Diels-Alder adducts

Chongchong Yang, Dandan Zhu, Chengyuan Sun, Buyun Chen, Yinghao Li, Indra Neel Pulidindi, Zhen Zheng, Xinling Wang

PII: S0266-3538(21)00123-8

DOI: https://doi.org/10.1016/j.compscitech.2021.108767

Reference: CSTE 108767

To appear in: *Composites Science and Technology*

Received Date: 17 November 2020

Revised Date: 13 February 2021

Accepted Date: 13 March 2021

Please cite this article as: Yang C, Zhu D, Sun C, Chen B, Li Y, Pulidindi IN, Zheng Z, Wang X, Electrothermal responsive self-healing for carbon fiber/epoxy interphase based on Diels-Alder adducts, *Composites Science and Technology*, https://doi.org/10.1016/j.compscitech.2021.108767.

CRedit Author Statement

Chongchong Yang: Conceptualization, Writing – Original Draft, Writing – Review & Editing; Methodology, Formal analysis, Investigation.

Dandan Zhu: Writing – Review $ Editing, Formal analysis, Investigation, Visualization.

Chengyuan Sun: Formal analysis, Investigation.

Buyun Chen: Writing – Review $ Editing;

Yinghao Li: Writing – Review $ Editing;

Indra Neel Pulidindi: Writing – Review $ Editing;

Zhen Zheng: Supervision, Validation.

Xinling Wang: Supervision, Resources, Project administration, Validation.

Graphical Abstract

Electrothermal responsive self-healing for carbon fiber/epoxy interphase based on Diels-Alder adducts

Chongchong Yang, Dandan Zhu, Chengyuan Sun, Buyun Chen, Yinghao Li, Indra Neel Pulidindi, Zhen Zheng, Xinling Wang*

School of Chemistry and Chemical Engineering, Frontiers Science Center for Transformative Molecules, State Key Laboratory of Metal Matrix Composites, Shanghai Jiao Tong University, Shanghai 200240, China

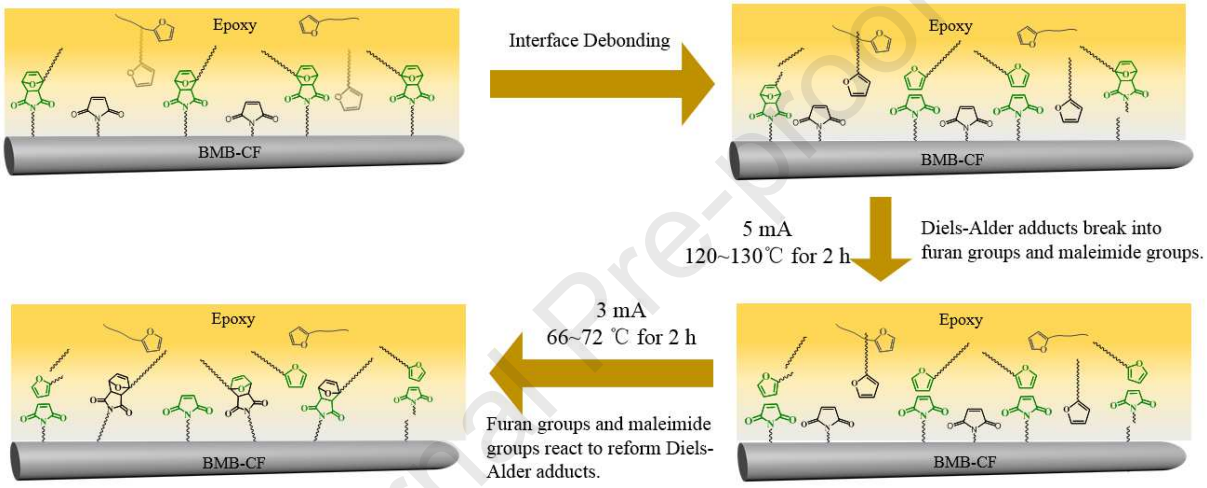

A more facile and more efficient self-healing strategy for fiber/epoxy (CF/EP) interphase was established based on electrothermal effect of CF driving the reversible transformation of covalent bonds. Diel-Alder (DA) cycloaddition adduct was introduced into the CF/EP interphase region to endow the interphase with thermoreversible covalent bonds. Based on the relationship between interphase temperature and electric current applied to carbon fiber, the interphase temperature was 66~72 ℃ and 120~130 ℃ when 3 mA and 5 mA was applied to carbon fiber composites, respectively. Therefore, 3 mA and 5 mA selected as the repairing electric current, and the treatment time was respectively 2 h. At 5 mA, the r-DA reaction occurred with the DA adducts broken up into furan groups and maleimide groups under the electrothermal effect of CFs. After the electric current decreased to 3 mA, the reversible covalent DA cycloaddition adducts could reform through the reaction between furan and maleimide groups under the electro thermal effect of CFs, which meant that the interphase was repaired. The optimized efficiency of the first and second healing was about 71.7 % and 41.1 %, respectively.

Electrothermally responsive self-healing for carbon fiber/epoxy interphase based on Diels-Alder adducts

Chongchong Yang, Dandan Zhu, Chengyuan Sun, Buyun Chen, Yinghao Li, Indra Neel Pulidindi, Zhen Zheng, Xinling Wang*

School of Chemistry and Chemical Engineering, Frontiers Science Center for Transformative Molecules, State Key Laboratory of Metal Matrix Composites, Shanghai Jiao Tong University, Shanghai 200240, China

Abstract

A more facile and more efficient self-healing strategy for carbon fiber/thermoset resin interphase was established based on electrothermal effect of carbon fiber (CF) driving the reversible transformation of covalent bonds. Diels-Alder cycloaddition adduct was introduced into the CF/epoxy (EP) interphase region to endow the interphase with thermoreversible covalent bonds through the oxidative co-polymerization and chemical surface grafting, which was nondestructive but more efficient. The modified carbon fiber was characterized via SEM, AFM, XPS and TGA. The CF/EP interphase temperature range in CF reinforced polymer composites (CFRPs) was adjusted through controlling the electric current applied to CFs according to the thermo-sensitivity of CF. The effect of electrothermal effect on the matrix resin around CFs was measured by micro-FTIR. The interfacial shear strength (IFSS) measurement verified that the electrothermal effect promoted the reversible transformation of the Diels-Alder cycloaddition adducts connecting the modified CFs with matrix resin, resulting in the self-healing behavior of the damaged interphase. This self-healing strategy not only can improve the interfacial adhesion of CFRPs without damages to the CF surface caused by the traditional oxidation modification methods, but also can reduce the possible heating aging and deformation of composites caused by convective thermal repairing methods. This strategy is a more efficient process.

Keywords: A. carbon fiber; A. CFRPs; A. Diels-Alder adduct; B. electrothermal effect; B. interphase self-healing

1. Introduction

In the past half century, the application of carbon fiber reinforced polymers (CFRPs) has achieved a dramatic increase in many fields, such as aerospace quality components, automotive frames, marine parts, war industry, construction industry, and so on. However, while the CFRPs are rapidly supplanting other types of materials, some special failure behaviors arise, for instance, delamination, debonding between fiber and matrix, fiber pull-out, interlaminar matrix cracking, hindering the application of CFRPs greatly[1-3]. As usual, most of these failures originate from micro-cracks born in interphase region of CFRPs. The micro-cracks, which are almost impossible to detect, grow deeper within polymeric materials, eventually resulting in unexpected performance reduction, such as mechanical degradation, electrical failure etc.[4, 5]. For a two component composite, the CF/matrix interphase plays a significant role in the integral properties of composite materials[6-9]. In order to fully realize the potential of CFRPs and guarantee the service security, technologies to prevent micro-cracks generation and propagation in the interphase region have to be developed, which has become a main subject in the field of CFRPs.

Inspired by self-healing capability of natural creatives, a range of approaches to endowing fiber reinforced composites with self-healing ability have been developed, including capsule-based[10-15], microvascular-based[16-19] or hollow fibers-based[20] delivery of healing agents, and thermally induced intrinsic healing[21-23]. Amanda R. J. prepared an autonomous recovery CF/epoxy interphases with a maximum healing efficiency of 91% through grafting micro-capsules containing reactive epoxy (EP) and ethyl phenyl acetate (EPA)[24]. Kumar C. N inserted macro-vascular tubes containing different healing agents into composites through VARTM processing, and found that the composites using vinyl ester (VE) and hybrid resin (HR) as healing agents presented high healing efficiency and mechanical properties[25]. However, despite of providing extra benefit of self-healing, the approaches based on enclosed healing agents presents some disadvantages[26-28]. For example, the incorporation of microcapsules or microvascular network compromises the structural integrity of composites, resulting in decrease of mechanical properties, and the microchannels within the composites

may act as initial sites of damage after healing agents being released. Zhen Hu introduced photothermal conversion nanoparticles into CFs surface to construct light-triggered self-healable interface based on photo-thermal effect in advanced composites[29, 30].

The thermoreversible characteristic of Diels-Alder bonds provides new opportunities for development of self-healing polymer and composites. Peterson incorporated Diels-Alder adducts into the glass fiber/ epoxy interphase region to create a remendable fiber-network interface[21]. Inspired by previous work, W. Zhang prepared thermally responsive self-healing interphase containing Diels-Alder adducts through maleimide-functionalized carbon fiber surface and furan-functionalized matrix resin[31].

As a resistive element, the conducting carbon fiber can provide heating in composites while the matrix resin acts as an insulator, which is applicable in the function design of CFRPs. E. Sancaktar et al. applied resistive electric heating via carbon fibers to tailor the interphase between carbon fiber/polymer, and found that the improvements obtained using resistive electric heating via carbon fibers was similar to those obtained by convective thermal postcure of the whole specimen[32]. This result proved the possibility of application of resistive electric heating via carbon fibers in interphase self-healing. Nathan Kwok introduced firstly electric resistive heating via carbon fibers network to repair composites[33]. Thereafter, the real healing of CFRPs via electric resistive heating method was demonstrated by Park[34-36].

However, most of studies on the application of electrothermal effect in self-healing composites focus on the healing of matrix resin or the interphase micro-cracks between carbon fiber and thermoplastic polymer. The application of electrothermal effect in repairing the fiber/thermoset resin interphase is still rarely reported, which is a tougher challenge. In this work, a novel electrothermally responsive self-healing strategy of CF/thermoset resin interphase was proposed. The reversible Diels-Alder cycloaddition adducts were introduced into the interphase region to endow the interphase region with thermoreversible covalent bonds. The thermo-sensitivity of CF and the relationship between resistance and electric current applied to CF was investigated, based on which the interphase temperature range was calculated.

The results showed that the interphase temperature could be adjusted from 66~130 ℃ through controlling the electric current applied to CFs in range of 3 mA ~ 5 mA. Hereby, 3 mA and 5 mA were selected as the repairing electric currents. The effect of electrothermal effect of CF on the interphase chemical component was characterized through micro-FTIR spectra. The IFSS measurement was conducted, confirming the electrothermally responsive interphase self-healing ability with first and second healing efficiency up to 71.7 % and 41.1 %, respectively. The interphase self-healing method proposed in this work was proved to be efficient.

2. Experiment

2.1 Raw materials

Polyacrylonitrile-based carbon fibers T700SC-24K series purchased from Toray Ltd. were used as reinforcing fibers, and epoxy-amine system provided by Shanghai Huayi resins Co., Ltd was used as the matrix resin. Dopamine (DA) hydrochloride was purchased from Sigma Aldrich. Hydroxylmethyl aminomethane (Tris), 1,6-bis(maleimide)butane (BMB), branched polyethyleneimine (PEI) with M_w= 600, N, N-Dimethylformamide (DMF) and acetonitrile was provided by Aladdin. 2-furanmethanamine (FA, purity 99%) and triethylamine (purity 99%) was purchased from Adamas. 2-furancarbonyl chloride was provided by Alfa. Acetone was purchased from Sinpharm Chemical Reagent Co., Ltd. Silver paint was purchased from Shenzhen Sinwe New Material Co., Ltd, and the curing process is at 60 ℃ for 1 h. All the chemical agents were used as received.

2.2 Surface modification

The graphitic structure of T700 series surface is very inert with no functional groups on surfaces available for direct chemical grafting[37, 38]. Thus, the surface treatment based on bio-inspired polyethyleneimine/polydopamine (PEI/PDA) hybrid layer method was conducted. The PEI/PDA co-deposition method not only could endow the CF surface with rich active groups, such as amine, secondary amine and hydroxyl groups, but also could avoid the damage to CF surface caused by traditional oxidation treatment, such as nitric acid oxidation, sul-

furic acid oxidation, ozone oxidation method, etc.[39-44]. CFs were firstly extracted by Soxhlet with acetone at 80 ℃ for 24 h to remove the sizing agent and pollutants on the surface, followed by being dried in a dry oven at 60 ℃ for 24 h. 1 M HCl was added to the aqueous solution containing 10 mM of Tris to adjust the pH value to 8.5. Then, PEI and DA were added to the buffer solution with a ratio of 4 mg: 2 mg: 1000 mL. The desized CFs were immersed into the PEI/DA solution for 24 h at room temperature. After being flushed with water, the PDA/PEI modified CFs were dried at 60 ℃ for 24 h. The modified CFs were denoted as NH_2-CF. Fig. 1 illustrated the detailed process of surface modification and functionalization for CFs.

After amine functionalization, furan groups, required for the further Diels-Alder reaction with maleimide groups, were grafted onto NH_2-CF via reaction with 2-furancarbonyl chloride at room temperature for 6 h with triethylamine as absorbent protons and drops of DMF as catalyst. The furan grafted CF was denoted as Furan-CF. Then the dried Furan-CF was put into excess acetonitrile solution of BMB and reacted at 60 ℃ for 6 h to obtain maleimide grafted CFs (denoted as BMB-CF), as shown in Fig. 1. The obtained BMB-CF was rinsed in excess acetonitrile to remove the unreacted BMB and dried at 60 ℃ overnight.

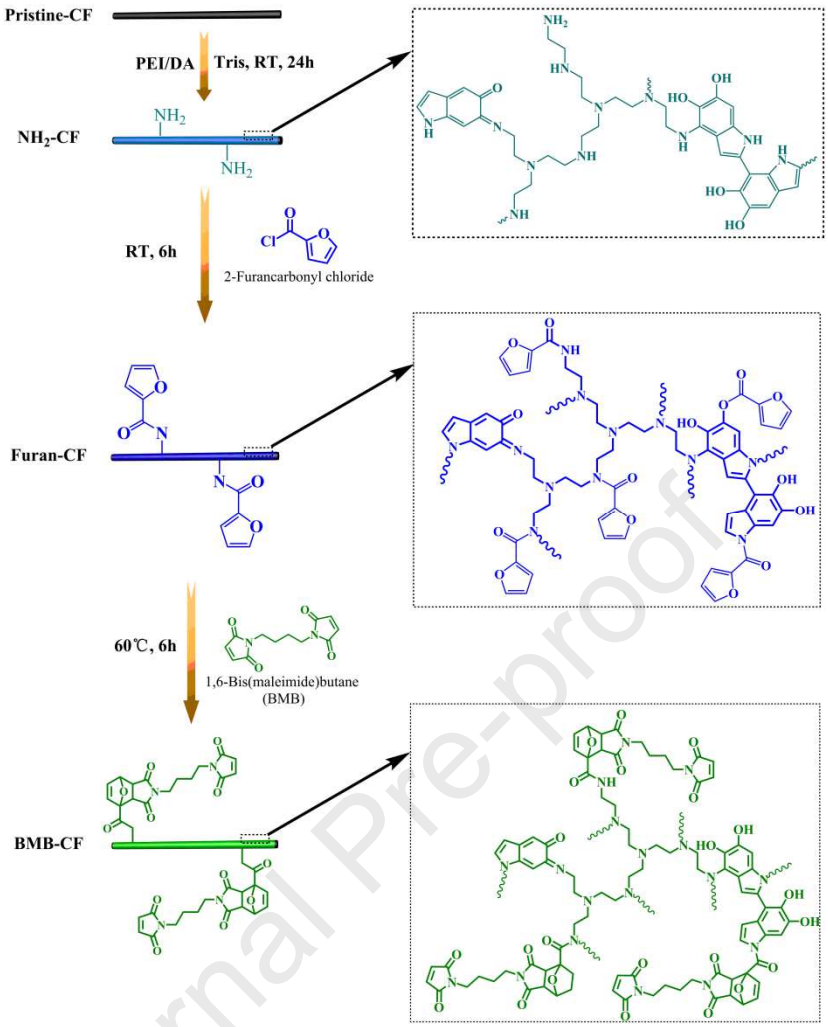

Figure 1. The surface modification and functionalization of CFs.

2.3 Preparation of specimens

To investigate the interfacial properties between CF and matrix resin, a micro-droplet method was conducted. In the preparation process of micro-droplet specimens, the ends of CF-monofilament were stuck on a specimen holder by heat-resisting tape. After epoxy resin were mixed with FA in weight ratio of 94:6, 87:13, 80:20 respectively, the mixture was deposited using a needle tip to process micro-droplets of mixture on CF-monofilament, as shown in Fig. S1. Then, the mixture droplets were cured as following three-step thermal treatment: 120 ℃ for 2 h, 150 ℃ for 2 h and 180 ℃ for 3 h. After curing process, the temperature was decreased to 60 ℃ slowly and kept at 60 ℃ for 2 h to allow the reformation of Diels-Alder adducts that separated at high temperature. The interfacial reaction and interfacial structure scheme were shown in Fig. S2. As reference, the micro-droplet specimens of un-

modified Pristine-CF/epoxy composites were also prepared.

Fig. S3 presented the CF-monofilament/epoxy composite specimen (Fig. S3a) and the specimen mold (Fig. S3b). In the preparation of CF-monofilament/epoxy composites, two copper plated electrodes were embedded into the ends of the cavity, then the ends of a CF-monofilament crossing through the grooves at the end of the mold were stuck on the mold with heat-resisting tape. The monofilament should be stretched axially by a 0.5 g weight before sticking in order that the monofilaments had a same initial stress. The carbon fibers were stuck on the copper plated electrodes with a silver paint to avoid large contact resistance. The mixture of epoxy components was slowly casted into the mold, and then was cured at 60 ℃ for 1 h, 120 ℃ for 2 h, 150 ℃ for 2 h and 180 ℃ for 3 h.

The CF-monofilament specimen shown in Fig. S4 was prepared by sticking the two ends of a CF-monofilament on a glass sheet. Firstly, two copper plated electrodes were stuck on a glass sheet. Then, the two ends of a CF-monofilament stretched axially by a 0.5 g weight were stuck on the copper plated electrodes with a silver paint. The copper plated electrodes and silver paint can avoid large contact resistance. At last, the CF-monofilament was placed at 60 ℃ for 1 h.

After being applied different electric current to, the specimens were cut perpendicularly to the carbon fiber axis into several rectangular specimens with a cross section of 3 mm × 2 mm, as shown by the wire-frame in Fig. S3a. The rectangular specimens were cut parallel to carbon fiber axis to expose a cross section, and this operation should make sure the carbon fiber would not be cut off. Then, the exposed cross section was mechanically grinded and polished parallel to the fiber axis on a polish-grinding machine (EM TXP, Leica). Polishing steps started with 800 grit grinding papers, followed by 2000, 5000 grit grinding papers, and then 0.25 μm alumina particles, until the surface of carbon fiber was exposed.

2.4 Characterization

2.4.1 Characterization of carbon fibers

The surface topography of CFs was investigated by scanning electron microscope (SEM, Nova NanoSEM 450, FEI, USA) and atom force microscope (AFM, Dimension Icon & Fast

Scan Bio, Bruker, Germany). SEM was conducted at 5 kV. The surface of carbon fibers was sputter-coated with gold (Q150TS, Quorum, UK) before observation. The probes used in AFM were silicon probes (AC240TS, Olympus, Japan) with resonant frequency about 70 kHz and spring constant of around 3 N/m. The scan range was 2 μm. Content of modifiers on surface of Pristine-CF and BMB-CF was assessed through thermogravimetric analysis (TGA, Discovery TGA550, TA, USA) in the range of 40-600 ℃ at heating rate of 10 ℃/min in a nitrogen atmosphere. The surface chemical elements and functional groups on carbon fiber surface were characterized thorough X-ray photoelectron spectroscopy (XPS, AXIS UltraDLD, Kratos, Japan) with pass energy of 160 eV and 40 eV for survey scans and narrow scans. The XPS was energy referenced to the C1s peak at 284.6 eV.

2.4.2 Resistance

The resistance of specimens at different electric currents was measured through a Precision Source (Keysight, B2901A). The electric currents applied to specimens were 0~9 mA. The resistance at different temperature was measured through electro chemical workstation (CHI 660E). Before measurement, the specimens were heated for 5-10 min in an oven to ensure the temperature of carbon fibers embedded in matrix resin was same as the environment temperature (i.e., the setting temperature). The temperature range was from 20 ℃ to 180 ℃.

2.4.3 Micro-FTIR spectra

Micro-FTIR spectra of the resin at different distance from carbon fibers were collected through Microscopes Fourier transform infrared (IR/iN10MX, Thermo Fisher). The scanning range was 4000-500 cm^{-1}, and the spot of laser beams was 10 μm × 50 μm. The light spot shifted perpendicularly to carbon fiber axis from carbon fibers to resin with the step size of 10 μm (as shown in Fig. 2). Then, the micro-FTIR spectra of resin at different distance from carbon fibers were recorded. The scanned zones were denoted as Zone 1~ Zone 10, respectively.

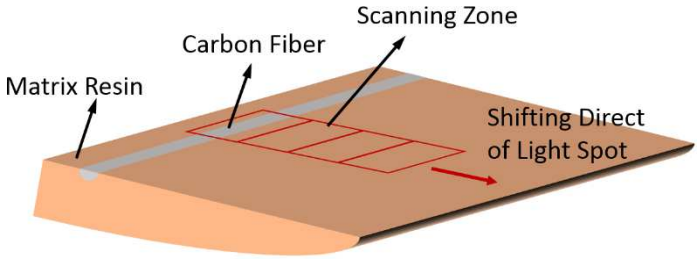

Figure 2. Schematic of micro-FTIR measurement.

2.4.4 Interfacial shear strength

Interfacial shear strength between CFs and matrix resin was characterized via micro-droplet method using an interfacial evaluation equipment (Beijing Future Material Sci-tech Co., Ltd, China). The displacement rate was 0.2 mm/min. The distance between two razor blades was 15 μm. IFSS was calculated as the following equation:

$$IFSS = \frac{P_m}{\pi dl} \quad \text{.....Equation (1)}$$

Where P_m is the peak applied force; d is the fiber diameter; l is the fiber length embedded in the matrix resin. At least 20 valid data were collected and averaged for each specimen.

2.4.5 Self-healing property

IFSS-displacement curves were important evidence to evaluate the interfacial self-healing properties of CF/EP composite micro-droplets. The micro-droplet method was conducted through pulling micro-droplets from carbon fiber surface. After a full interfacial debonding, the debonded micro-droplet specimens were loaded with 5 mA electric current for 2 h by a Precision Source (Keysight, B2901A) so that the retro-Diels-Alder reaction occurred. The electric current was decreased and kept at 3 mA for 2 h to conduct Diels-Alder reaction between furan and maleimide groups to reform new Diels-Alder adducts, which meant the completion of first self-healing treatment. After that, the second micro-droplet method was conducted to evaluate the IFSS-displacement curves. This test also meant the completion of the second full interfacial debonding. Till then, the first healing-debonding cycle finished, and after that the second healing-debonding cycle started. At least 20 valid data were collected and averaged for each specimen.

The interfacial healing efficiency (f) was calculated as the following equation:

$$f_i = L_{hi} / L_0 \quad (i=1, 2, 3, 4\ldots) \qquad \ldots\ldots\ldots\ldots\ldots\ldots (2)$$

Where L_{hi} was the maximum IFSS of healed specimens in each healing-debonding cycle; L_0 was the maximum IFSS of initial specimens.

3. Results and discussions

3.1 Characterization of surface-modified carbon fiber

3.1.1 Surface topography

SEM and AFM were used to monitor the surface topography evolution of carbon fibers during the modification process. The SEM and AFM topographies were respectively shown in Fig. 3 and Fig. 4. The surface of Pristine-CF was typically smooth and neat. After immersion in fresh DA/PEI solution, the surface of resultant PDA-PEI-CF was uniformly covered with a rough thin layer, which was considered as the PDA/PEI co-deposition coating. The layer of PDA/PEI could provide more reactive sites for subsequent grafting reaction. After grafting reaction with 2-furancarbonyl chloride and subsequent BMB, the thin coating layer became impact and thicker, as shown in Fig. 3c. The AFM topographies indicated the BMB-CFs had rougher surface than Pristine-CFs and PDA-PEI-CFs. The improvement of surface roughness would result in bigger surface area and more intense mechanical interlocking effect between the fibers and matrix, which was expected to improve the interphase adhesion.

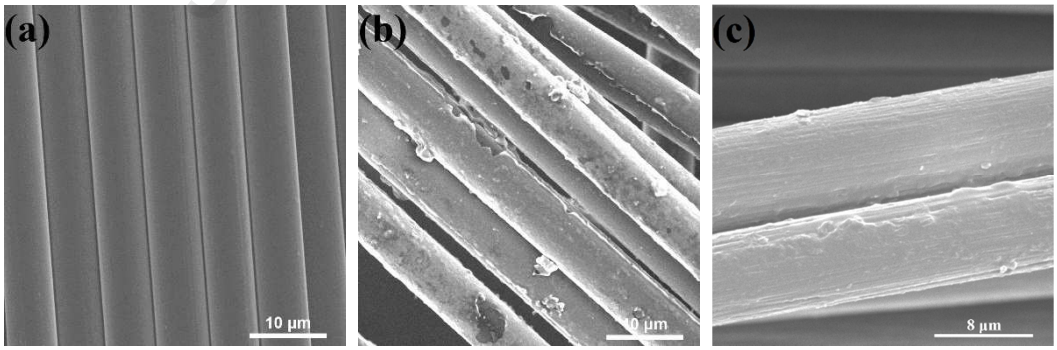

Figure 3. SEM topography of different carbon fibers. a: Pristine-CF; b: PDA-PEI-CF; c: BMB-CF.

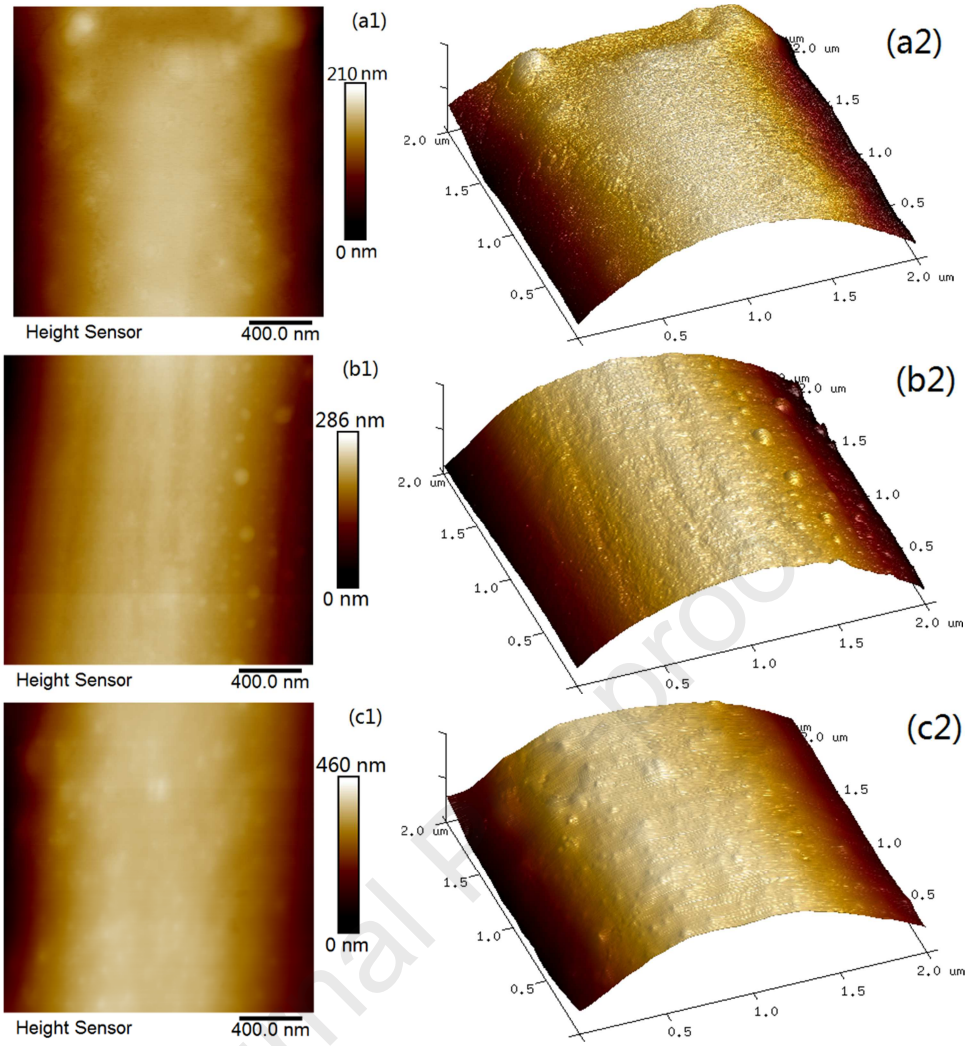

Figure 4. AFM topography of different carbon fibers. a1, a2: Pristine-CF; b1, b2: PDA-PEI-CF; c1, c2: BMB-CF.

3.1.2 Content of surface modifiers

The thermogravimetric analysis (TGA) was used to evaluate the content of the surface modifiers that grafted onto CF surface. The TGA curves of Pristine-CF and BMB-CF were shown in Fig. 5. Pristine-CFs showed 0.96 % weight loss, which could be ascribed to the thermal decomposition of the sizing agent on the surface of Pristine-CFs. The weight loss of the BMB-CF was about 2.5 %, which could be ascribed to the thermal decomposition of the modifier on the surface of BMB-CFs. Therefore, the TGA curves suggested the presence of modifiers on BMB-CFs surface.

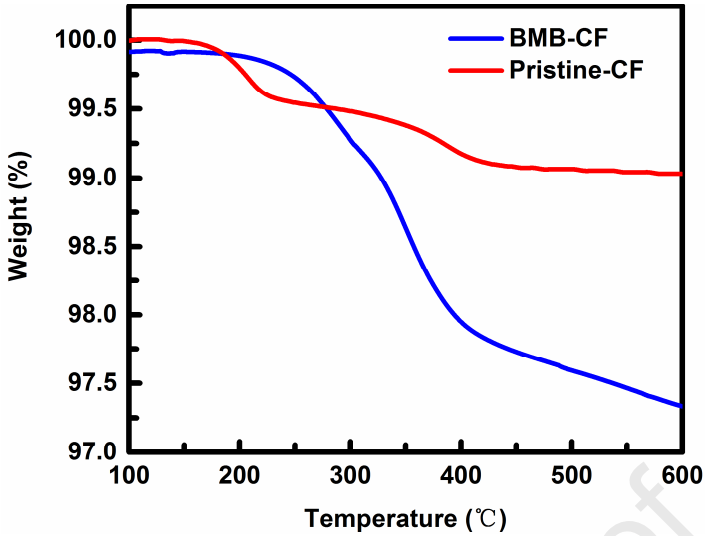

Figure 5. TGA curves of Pristine-CF and BMB-CF.

3.1.3 Modified carbon fiber surface chemical component

XPS was a highly sensitive analysis instrument for chemical elements. In this work, to confirm the successful grafting of modifiers on carbon fiber surface, XPS was performed to detect the chemical component and chemical environment on BMB-CF surface. The XPS survey spectrum was shown in Fig. 6a. The peaks around 284.8 eV, 400.5 eV and 532.8 eV in the wide-scan XPS spectrum of BMB-CFs could be attributed to C1s, N1s and O1s, respectively, suggesting that the main elements were carbon, oxygen and a small amount of nitrogen. The content of C, O, N was about 74.3 %, 18.8% and 6.9 %, respectively. To obtain more component information of the modified carbon fibers, the narrow-scan spectrum of O1s was fitted into C=O (531.1-531.9 eV), C-OH (532.3-532.6 eV), C-O-C (533.2-533.7 eV) based on the chemical environment of oxygen through peak deconvolute method using a Gaussian multipeak fit, as shown in Fig. 6b. The percent of C=O, C-OH, C-O-C was 11.3 %, 58.4 %, 30.3 %, respectively.

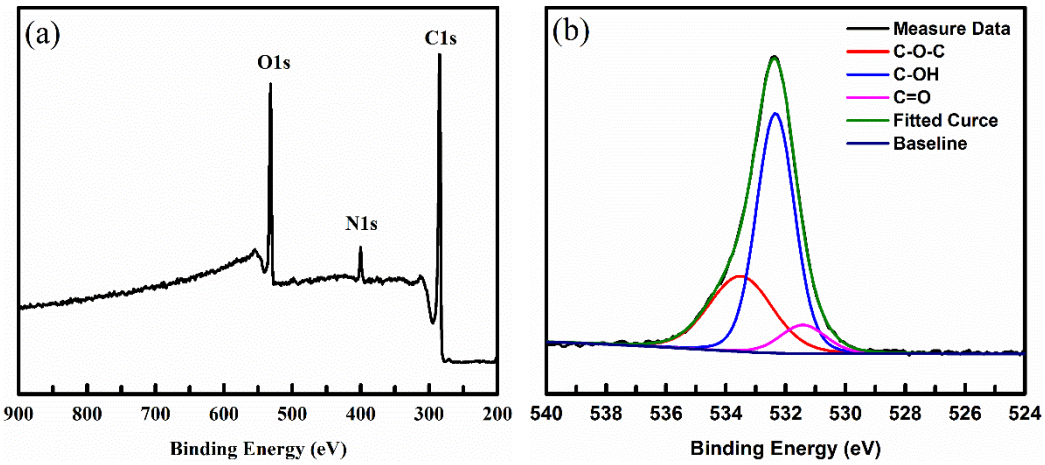

Figure 6. XPS survey spectrum of BMB-CFs and curve fitting for O1s peak.

3.2 Electrothermally responsive interphase

It was hard to immediately measure the interphase temperature due to the micro-scale interphase region with the thickness of tens to several hundred nanometers[45-47]. Thus, this work used a theoretical derivation method, which was based on the corresponding relationship between the temperature and the electric current at an identical resistance value.

The resistance per unit length (denoted as RPL, Ω/mm) of CF-monofilaments and CF-monofilament/epoxy composites at different temperature was shown in Fig. 7a. The resistance of both CF-monofilaments and CF-monofilament/epoxy composites decreased as the temperature increased, presenting significant negative temperature coefficient (NTC). Similarly, as the electric current increased, the resistance also decreased, as shown in Fig. 7b. Carbon fiber T700 had a negative thermal expansion coefficient (CTE, about -0.38×10^{-6} /℃). Namely, the carbon fiber showed axial shrinkage when heated. According to the equation $R=\rho \times L/S$, the axial shrinkage of the CF-monofilament caused by the increasing temperature resulted in the reduction of resistance (R) of CF. The CTE of the matrix resin was about $(50\sim70) \times 10^{-6}$ /℃, which meant the matrix resin showed volume expansion when heated. For the CF-monofilament/EP composites, the thermal shrinkage of CF-monofilament embedded in the matrix resin was limited by the thermal expansion of the matrix resin. Therefore, the carbon fiber in composites presented a weak negative temperature coefficient and higher resistance comparing with CF-monofilament at same temperature.

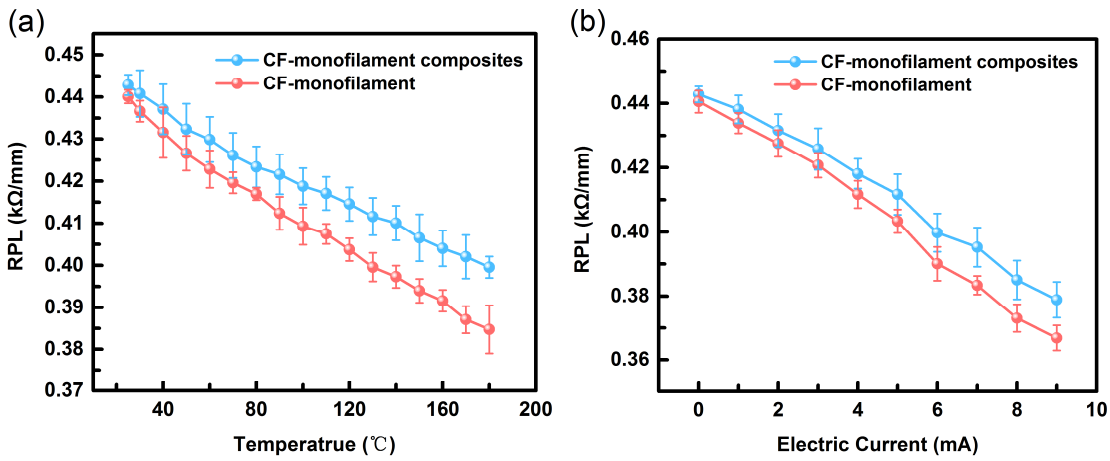

Figure 7. (a) Temperature sensitive effect curves of CF-monofilament and CF-monofilament composites; (b) The relationship curves between RPL of CF-monofilament and CF-monofilament composites and electric current.

For CF-monofilament/EP composites, the convective heating and electric resistance heating were different heating modes. In convective heating mode, the heat was transformed from environment (air in oven) to matrix resin, then to CFs, and the temperature field in matrix and CFs was considered homogeneous. Thus, the interphase temperature could be deemed to be identical to the environment temperature. In electric resistance heating mode, the heat was transformed from CF (heat source) to matrix resin, then to environment. Thus, in electric resistance heating mode, the interphase temperature (T_{interp}) was lower than the temperature (T_{mce}) of CF-monofilament in composites, and higher than the temperature (T_{mre}) of the matrix resin, i.e., $T_{mre} < T_{interp} < T_{mce}$, which meant the temperature gradient existed in CF-monofilament composites.

For CF-monofilament composites heated by electric current, the thermal expansion of matrix resin would restrict the thermal shrinkage of CF-monofilament. If the CF-monofilament and CF-monofilament composites were applied same electric current to, according to the equation $R=\rho \times L/S$, the resistance (R_{mce}) of CF-monofilament composites heated by electric current was larger that (R_{me}) of CF-monofilament heated by same electric current, i.e., $R_{mce} > R_{me}$, as shown in Fig. 7b. The higher resistance meant CF-monofilament produced more heat in composites. Thus, the temperature (T_{mce}) of CF-monofilament in composites was considered higher than that (T_{me}) of CF-monofilament heated by same elec-

tric current. Due to the micro-scale interphase region with the thickness of tens to several hundred nanometers, the temperature of interphase was considered relatively close to that of CF-monofilament in composites. Therefore, the interphase temperature (T_{interp}) was considered higher than the surface temperature (T_{me}) of CF-monofilament heated by same electric current, i.e., $T_{me} < T_{interp}$. Based on the above analysis, the following relationship could be obtained: $T_{me} < T_{interp} < T_{mce}$. It meant it was considered that the relationship curve of interphase temperature and electric current in composite should similarly lie between curves for CF-monofilament and CF-monofilament composites.

Based on the corresponding relationship between the temperature and the electric current at an identical resistance value, the relationship curves between the temperature of the specimens and the electric current applied to the specimens were obtained, as shown in Fig. 8. The temperature in the interphase region was considered to fall into the shadow region in Fig. 8. From Fig. 8, as the electric current of 3 mA and 5mA was applied to specimens, the interphase temperature should be 66~72 ℃ and 120~130 ℃, respectively. Usually, the temperature of Diels-Alder reaction and retro-Diels-Alder reaction was 50-70 ℃ and 90-130 ℃, respectively[23, 34]. Therefore, the electric current of 3 mA and 5mA was selected as the repairing electric current. The interphase repairing processing was as follows: 5 mA for 2 h, and 3 mA for 2 h.

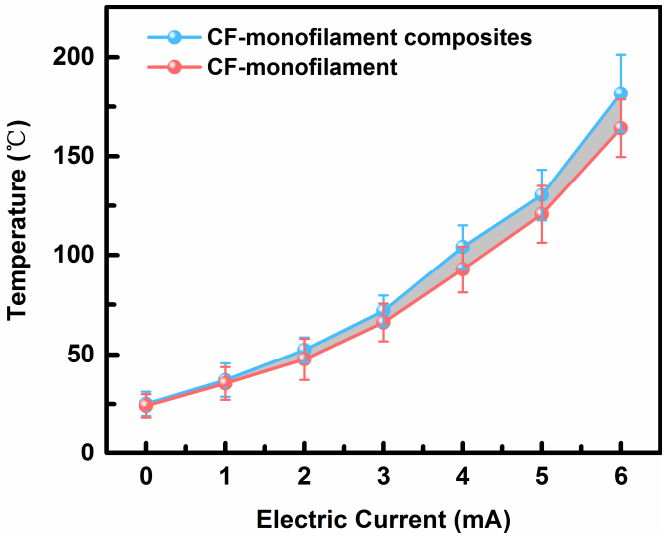

Figure 8. The relationship between the interphase temperature and the electric current applied to carbon fibers.

3.3 Effect of electric-thermal on chemical compositions in interphase region

The effect of electrothermal effect on the chemical compositions of the resin adjacent to CF was investigated through micro-FTIR. The micro-FTIR spectra of the resin adjacent to CF were shown in Fig. S5, and the micro-FTIR spectra of the epoxy groups (917 cm^{-1}) were shown in Fig. 9. The transmittance of epoxy groups decreased with the increase of the distance from CF, indicating that the conversion rate of epoxy groups increased as the distance of resin from CF decreased. The results showed that the electrothermal effect promoted the postcure of resin adjacent to CF, and the promotion effect was similar to convective heating. Moreover, the electrothermal effect showed significant locality, and only the resin in the localization region could be heated effectively. It verified the feasibility of electrothermal effect of CF to be used for repairing the damaged interphases in CFRPs.

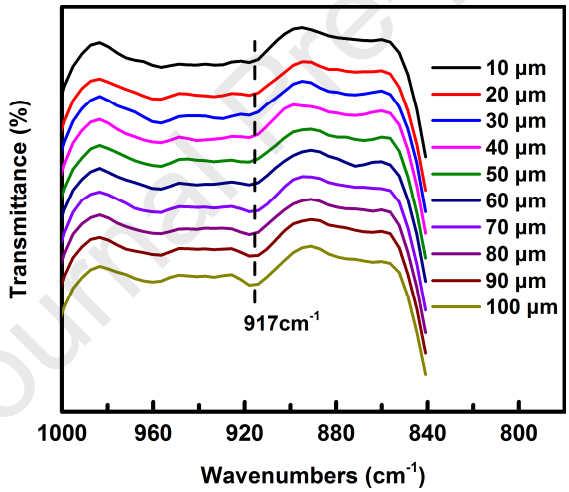

Figure 9. The micro-FTIR spectra of resin with different distance from CF treated by electric reistance heating.

3.4 Electrothermally responsive interphase self-healing

3.4.1 Interfacial debonding and self-healing

The Diels-Alder cycloaddition adduct was more fragile than other covalent bonds in a polymer chain[34]. Therefore, in the process of interfacial debonding, the Diels-Alder adducts were much easier to break up under excessive load. At 5 mA, the interphase temperature increased to 120-130 ℃, and the retro-Diels-Alder reaction occurred with the Diels-Alder adducts broken up into furan groups and maleimide groups under the electrothermal effect of

CFs[23, 34, 48]. After the electric current decreased to 3 mA, the interphase temperature decreased to 66~72 ℃, and the reversible covalent Diels-Alder cycloaddition adducts could reform through the reaction between furan and maleimide groups under the electrothermal effect of CFs, which meant that the interphase was repaired. The furan and maleimide groups were mainly from the retro-Diels-Alder reaction, and a little portion were the residual ones. The mechanism of interphase debonding and healing was shown in Fig. 10.

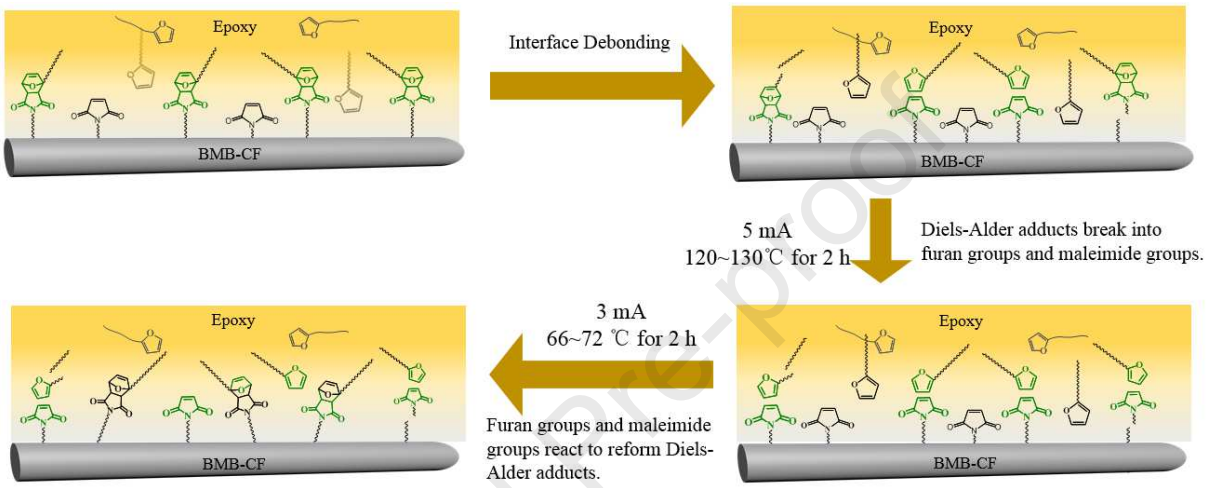

Figure 10. Mechanism of interphase debonding and self-healing.

Self-healing properties of the CF/EP interphase were evaluated by repeated debonding-healing test of micro-droplet specimens. Representative load-displacement curves of self-healing specimens and control specimens were shown in Fig. 11. The self-healing specimens and control specimens were treated under same conditions: 5 mA (120~130 ℃ of interphase temperature) for 2h and then 3 mA (66~72 ℃ of interphase temperature) for 2h. In loading process, the load dropped suddenly and reached a frictional plateau after the micro-droplet was loaded to a certain maximum value. At the point where the load reached the maximum value, the full interfacial debonding occurred. The maximum value was defined as debonding force, and the force in frictional plateau was considered as frication force between micro-droplets and carbon fiber surfaces.

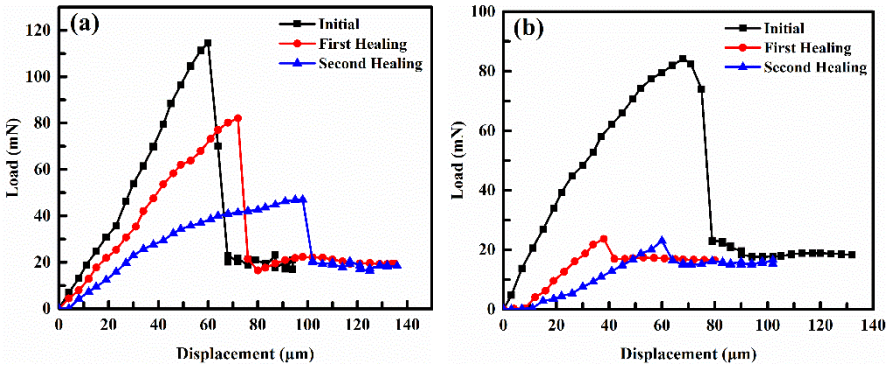

Figure 11. Representative load-displacement curves of (a) self-healing (BMB-CF/EP composites) specimen with recovery of IFSS and (b) control (Pristine-CF/EP composites) specimen with recovery of only frictional force.

From Fig. 11a, the self-healing specimen was loaded to 114.6 mN before the first full interfacial debonding, and then the load quickly reached the frictional plateau (about 16.7 mN). After the first and second self-healing treatments, the micro-droplet test of the identical specimen was carried out again, and the maximum debonding forces reached 82.1 mN and 47.0 mN, respectively, which demonstrated that the Diels-Alder adducts broken up in the process of interfacial debonding were reformed successfully in the self-healing treatment (5 mA (120~130 ℃ of interphase temperature) for 2h and then 3 mA (66~72 ℃ of interphase temperature) for 2h), and the interfacial adhesion was improved. However, in contrast, after the first and second self-healing, the control specimen (Pristine-CF/EP composites) only recovered the friction force. The difference between the load-displacement curves of the self-healing specimen and the control specimen demonstrated the successful application of electrothermal effect in the CF/EP interphase self-healing.

In order to further verify the self-healing behavior, the SEM topographies of different composite micro-debonding specimens prior and after healing process were observed, as shown in Fig. 12. Obviously, both of pristine-CFs and BMB-CFs were completely intact with epoxy resin before debonding process, as shown in Fig 12 a1 and b1. After debonding process, an apparent micro-crack appeared between fibers and epoxy resin, as shown in Fig. 12 a2 and b2. After healing process, the micro-cracks presented no obvious change as shown by SEM topographies of Pristine-CF/EP composite micro-droplets in Fig. 12 a3. However, the micro-cracks disappeared, and the more intense interaction between BMB-CFs and epoxy resin

reformed after healing process as shown by the SEM topographies of BMB-CF/EP composite micro-droplets in Fig. 12 b3. It indicated the interphase between BMB-CFs and epoxy was newly reformed after healing process. After the second healing process, the interphase was reformed again, as shown in Fig. 12 c2, indicating complete healing of interphase micro-cracks.

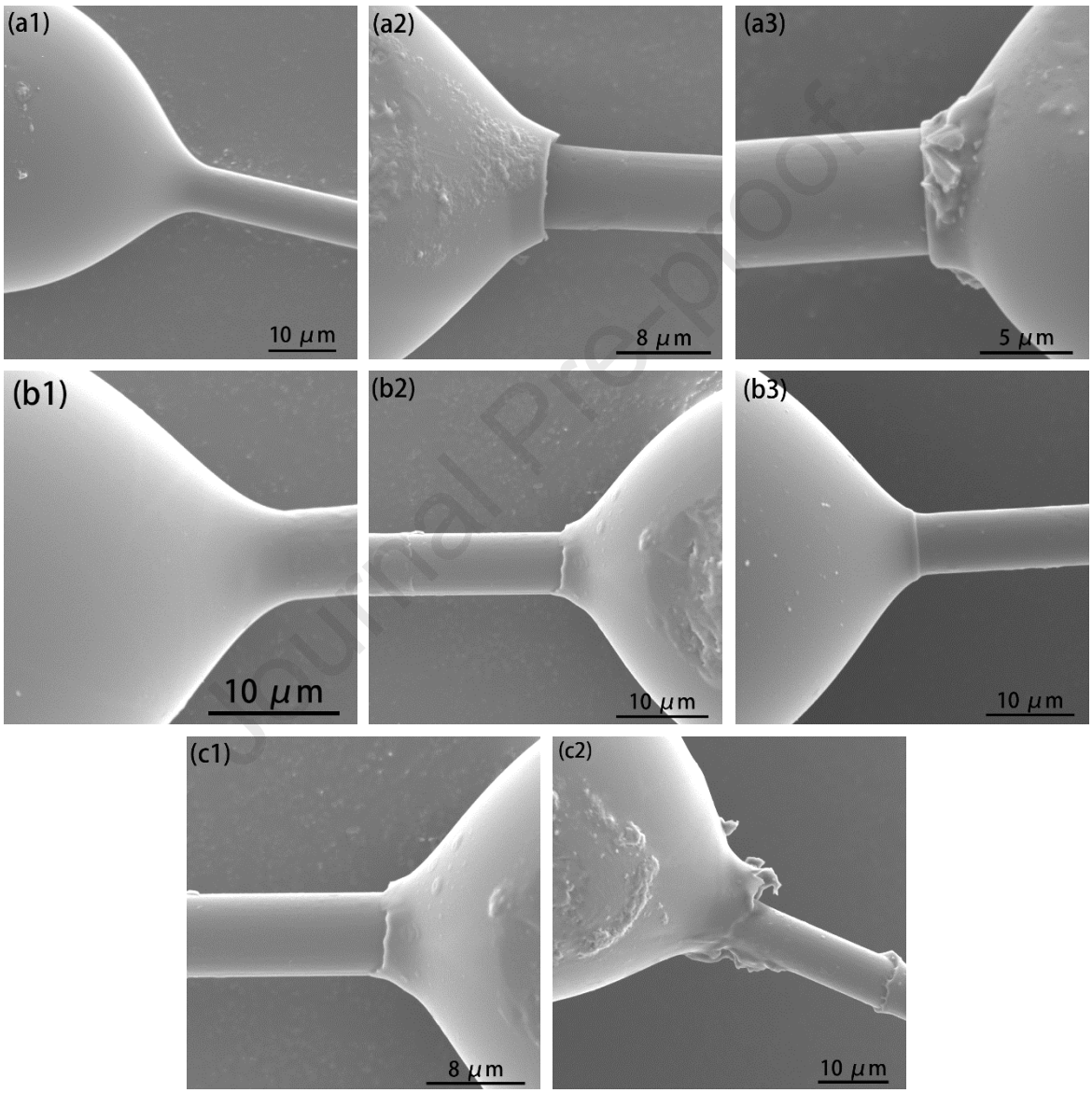

Figure 12. SEM topographies of different micro-droplet specimens. (a1), (a2), (a3): initial, debonded and healed Pristine-CF/EP composites specimen; (b1), (b2), (b3), (c1) (c2): initial, first debonded, first healed, second debonded and second healed BMB-CF/EP composites specimen.

3.4.2 Interfacial healing efficiency

Micro-droplet method was used to characterize the IFSS between CFs and resin matrix.

Fig. 13 showed the micro-debonding test results of control (Pristine-CF/EP composites) specimens and self-healing (BMB-CF/EP composites) specimens with different content of FA in matrix. It can be seen that the self-healing specimens containing FA in matrix had higher IFSS than control specimens. For self-healing specimens containing 13% of FA in matrix, the IFSS value was 68.49 MPa, 51.12 % higher than 45.32 MPa of control specimens. The improved IFSS showed that the interfacial adhesion properties between CFs and epoxy was improved by the BMB functionalization of CFs, which could be ascribed to the formation of more chemical interaction bonds and mechanical interlocking between CF and epoxy. Meanwhile, some pieces of epoxy matrix remaining on carbon fiber surface after debonding also indicated the improved interfacial adhesion, as shown in Fig. 12 b2.

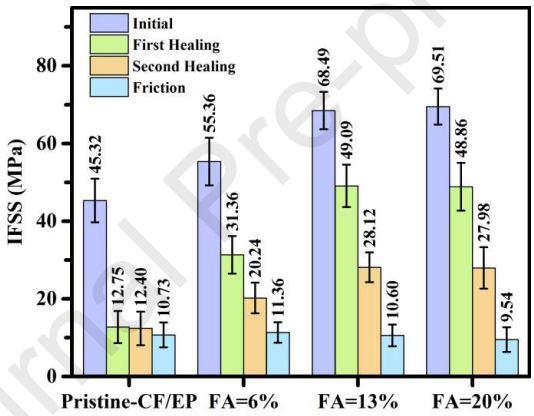

Figure 13. IFSS of self-healing (BMB-CF/EP composites) specimens with different content of FA in matrix and control (Pristine-CF/EP composites) specimen after healing.

As reference, the IFSS of the first and second healed control specimen was 12.75 MPa and 12.40 MPa, respectively, almost equal to the friction between micro-droplets and carbon fiber surface. By comparison, it can be found that after the first and second healing treatment the IFSS of self-healing specimens was much higher than that of control specimens, which should be attributed to the reformation of the chemical bonds, Diels-Alder bonds, connecting matrix resin and carbon fibers. It suggested that the damaged interphase was successfully healed under the electrothermal effect, consistent with the analysis results in section 3.4.1.

Fig. 14 showed the healing efficiency of self-healing (BMB-CF/EP composites) specimens and control (Pristine-CF/EP composites) specimens. The optimized efficiency of the first and second healing was about 71.7 % and 41.1 %, respectively. For control specimens,

the healing efficiency of the first healing and the second healing treatment was 27.3 % and 27.7 %, respectively. However, it should be noted that the self-healing efficiency of Pristine-CF/EP composites should be attributed to friction forces generated from sliding of the matrix droplets on the surface of carbon fibers, not the self-healing effect. For self-healing specimens, the healing efficiency increased as the content of FA in matrix increased, attributed to that the increase of FA in matrix brought the formation of more Diels-Alder adducts in interphase region. The electrothermal effect responsive interphase self-healing method presented a similar healing effect to the convective thermal repairing method reported by W. Zhang[31, 48].

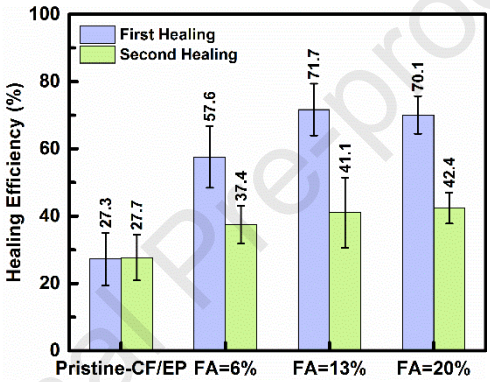

Figure 14. Healing efficiency of self-healing (BMB-CF/EP composites) specimens with different content of FA in matrix and control (Pristine-CF/EP composites) specimen.

As shown in Fig. 14, the healing efficiency decreased as the debonding times increased. On one hand, although Diels-Alder adducts were more likely to be broken and generate furan groups and maleimide groups under excessive load, partial Diels-Alder adducts were still separated asymmetrically, which led to the reduction in furan groups and maleimide groups in interphase region. On the other hand, relative sliding between micro-droplets and surface of CFs caused the generation of micro-gaps between micro-droplets and surface of CFs. The relatively deep micro-gaps (as shown in Fig. 12 c2) prevented the reaction of furan groups and maleimide groups, which reduced the interfacial healing ability. As the debonding-healing cycles increased, the effects accumulated step by step led to the decrease in the promotion effect of the electrothermal effect on the self-healing efficiency.

4. Conclusion

In this work, electrothermal effect of carbon fibers has been used to successfully repair the CF/EP interphase containing thermoreversible covalent bonds, which was more facile and more efficient. The resistance of carbon fibers decreased as the temperature and electric current increased, presenting negative temperature coefficient, based on which the interphase temperature has been evaluated. The micro-FTIR spectra indicated that electric resistance heating presented promotive effect on the reactions around carbon fibers in composites, similarly to convective heating. The damaged Diels-Alder cycloaddition adducts in interphase region reformed under the response of electric resistive heating of carbon fibers in CFRPs. The micro-droplet measurement verified the self-healing behavior of the damaged interphase, and the SEM topographies suggested the disappearance and reformation of interphase micro-cracks before and after healing treatment. The optimized efficiency of the first and second healing was about 71.7 % and 41.1 %, respectively. The electrothermally responsive interfacial self-healing technique not only could avoid the damages to the CF surface caused by the traditional oxidation modification methods, but also could reduce the heating aging of the matrix resin and deformation of composites caused by convective thermal repairing methods.

More future work will focus on optimization research on the effect of some factors on the self-healing ability, such as the modification methods, the self-healing conditions, et al..

References:

[1] J.G. Njiri, N. Beganovic, et al., Consideration of lifetime and fatigue load in wind turbine control, Renew. Energ. 131 (2019) 818-828.

[2] J. Zhao, S. Yan, et al., Design and analysis of biomimetic nose cone for morphing of aerospace vehicle, J. Bionic Eng. 14(2) (2017) 317-326.

[3] W.J. Cantwell, J. Morton, The significance of damage and defects and their detection in composite materials: A review, The journal of strain analysis for engineering design 27(1) (1992) 29-42.

[4] E.K. Gamstedt, R. Talreja, Fatigue damage mechanisms in unidirectional carbon-fibre-reinforced plastics, J. Mater. Sci. 34(11) (1999) 2535-2546.

[5] J. Renard, A. Thionnet, Damage in composites: From physical mechanisms to modelling, Compos. Sci. Technol. 66(5) (2006) 642-646.

[6] H. Rahmani, A. Ashori, et al., Surface modification of carbon fiber for improving the interfacial adhesion between carbon fiber and polymer matrix, Polym. Advan. Technol. 27(6) (2016) 805-811.

[7] M. Sharma, S. Gao, et al., Carbon fiber surfaces and composite interphases, Compos. Sci. Technol. 102 (2014) 35-50.

[8] E. Totry, J.M. Molina-Aldareguía, et al., Effect of fiber, matrix and interface properties on the in-plane shear deformation of carbon-fiber reinforced composites, Compos. Sci. Technol. 70(6) (2010) 970-980.

[9] Z. Serge, E. Mäder, Characterization of fiber/matrix interface strength: Applicability of different tests, approaches and parameters, Compos. Sci. Technol. 65(1) (2005) 149-160.

[10] H. Ullah, K.A. M Azizli, et al., The potential of microencapsulated self-healing materials for microcracks recovery in self-healing composite systems: A review, Polym. Rev. 56(3) (2016) 429-485.

[11] Y. Tao, Y. Chang, et al., Self-healing Ag/epoxy electrically conductive adhesive using encapsulated epoxy-amine healing chemistry, J. Appl. Polym. Sci. 132(7) (2015).

[12] H. Jin, C.L. Mangun, et al., Self-healing thermoset using encapsulated epoxy-amine healing chemistry, Polymer 53(2) (2012) 581-587.

[13] J.L. Moll, S.R. White, et al., A self-sealing fiber-reinforced composite, J. Compos. Mater. 44(22) (2010) 2573-2585.

[14] B.J. Blaiszik, M. Baginska, et al., Autonomic recovery of Fiber/Matrix interfacial bond strength in a model composite, Adv. Funct. Mater. 20(20) (2010) 3401.

[15] S.H. Cho, H.M. Andersson, et al., Polydimethylsiloxane-Based Self-Healing materials, Adv. Mater. 18(8) (2006) 997-1000.

[16] J.F. Patrick, K.R. Hart, et al., Continuous Self-Healing life cycle in vascularized structural composites, Adv. Mater. 26(25) (2014) 4302-4308.

[17] A.R. Hamilton, N.R. Sottos, et al., Pressurized vascular systems for self-healing materials, J. R. Soc. Interface 9(70) (2012) 1020-1028.

[18] A.R. Hamilton, N.R. Sottos, et al., Self-Healing of internal damage in synthetic vascular materials, Adv. Mater. 22(45) (2010) 5159-5163.

[19] C.J. Hansen, W. Wu, et al., Self-Healing materials with interpenetrating microvascular networks, Adv. Mater. 21(41) (2009) 4143-4147.

[20] S. Zainuddin, T. Arefin, et al., Recovery and improvement in low-velocity impact properties of e-glass/epoxy composites through novel self-healing technique, Compos. Struct. 108 (2014) 277-286.

[21] A.M. Peterson, R.E. Jensen, et al., Thermoreversible and remendable glass‐polymer interface for fiber-reinforced composites, Compos. Sci. Technol. 71(5) (2011) 586-592.

[22] P. Cordier, F. Tournilhac, et al., Self-healing and thermoreversible rubber from supramolecular assembly, Nature 451(7181) (2008) 977-980.

[23] X. Chen, M.A. Dam, et al., A thermally re-mendable Cross-Linked polymeric material, Science 295 (2002) 1698-1702.

[24] A.R. Jones, A. Cintora, et al., Autonomic healing of carbon Fiber/Epoxy interfaces, ACS Appl. Mater. Inter. 6(9) (2014) 6033-6039.

[25] C. Naga Kumar, M.N. Prabhakar, et al., Result of vascular tube design on the curative and mechanical performance of modified carbon fibers/hybrid resin self‐healing composites, Polym. Composite. 41(5) (2020) 1913-1924.

[26] A. Ghaemi, A. Philipp, et al., Mechanical behaviour of micro-capsules and their rupture under compression, Chem. Eng. Sci. 142 (2016) 236-243.

[27] K. Van Tittelboom, N. De Belie, et al., Self-healing efficiency of cementitious materials containing tubular capsules filled with healing agent, Cement and Concrete Composites 33(4) (2011) 497-505.

[28] K.S. Toohey, N.R. Sottos, et al., Self-healing materials with microvascular networks, Nat. Mater. 6(8) (2007) 581-585.

[29] Q. Shao, Z. Hu, et al., Mussel-inspired immobilization of BN nanosheets onto poly(p-phenylene benzobisoxazole) fibers: Multifunctional interface for photothermal self-healing, Appl. Surf. Sci. 440 (2018) 1159-1165.

[30] Z. Hu, Q. Shao, et al., Light triggered interfacial damage self-healing of poly(p-phenylene benzobisoxazole) fiber composites, Nanotechnology 29(18) (2018) 185602.

[31] W. Zhang, J. Duchet, et al., Effect of epoxy matrix architecture on the self-healing ability of thermo-reversible interfaces based on Diels-Alder reactions: Demonstration on a carbon fiber/epoxy microcomposite, RSC Adv. 6(115) (2016) 114235-114243.

[32] E. Sancaktar, W. Ma, et al., Electric resistive heat curing of the Fiber-Matrix interphase in Graphite/Epoxy composites, J. Mech. Design 115(1) (1993) 53-60.

[33] N. Kwok, H.T. Hahn, Resistance heating for self-healing composites, J. Compos. Mater. 41(13) (2007) 1635-1654.

[34] J.S. Park, T. Darlington, et al., Multiple healing effect of thermally activated self-healing composites based on Diels–Alder reaction, Compos. Sci. Technol. 70(15) (2010) 2154-2159.

[35] J.S. Park, H.S. Kim, et al., Healing behavior of a matrix crack on a carbon fiber/mendomer composite, Compos. Sci. Technol. 69(7-8) (2009) 1082-1087.

[36] J.S. Park, K. Takahashi, et al., Towards development of a Self-Healing composite using a mendable polymer and resistive heating, J. Compos. Mater. 42(26) (2008) 2869-2881.

[37] M.C. Paiva, C.A. Bernardo, et al., Mechanical, surface and interfacial characterisation of pitch and PAN-based carbon fibres, Carbon 38(9) (2000) 1323-1337.

[38] Y. Huang, R.J. Young, Effect of fiber microstructure upon the modulus of PAN- and Ptich- based carbon fibers, Carbon 33(2) (1995) 97-107.

[39] X. Yuan, B. Zhu, et al., Influence of different surface treatments on the interfacial adhesion of graphene oxide/carbon fiber/epoxy composites, Appl. Surf. Sci. 458 (2018) 996-1005.

[40] Y. Liu, Y. Fang, et al., Mussel-inspired modification of carbon fiber via polyethyleneimine/polydopamine co-deposition for the improved interfacial adhesion, Compos. Sci. Technol. 151 (2017) 164-173.

[41] L. Meng, D. Fan, et al., The effect of oxidation treatment by KClO3/H2SO4 system on intersurface performance of carbon fibers, Appl. Surf. Sci. 268 (2013) 225-230.

[42] S. Chen, Y. Cao, et al., Polydopamine as an efficient and robust platform to functionalize carbon fiber for High-Performance polymer composites, ACS Appl. Mater. Inter. 6(1) (2013) 349-356.

[43] S.Y. Kim, S.J. Baek, et al., New hybrid method for simultaneous improvement of tensile and impact properties of carbon fiber reinforced composites, Carbon 49(15) (2011) 5329-5338.

[44] S. Tiwari, J. Bijwe, et al., Tribological studies on polyetherimide composites based on carbon fabric with optimized oxidation treatment, Wear 271(9-10) (2011) 2252-2260.

[45] Y. Liu, D. He, et al., Comparison of different surface treatments of carbon fibers used as reinforcements in epoxy composites: Interfacial strength measurements by in-situ scanning electron microscope tensile tests, Compos. Sci. Technol. 167 (2018) 331-338.

[46] L. Liu, C. Jia, et al., Interfacial characterization, control and modification of carbon fiber reinforced polymer composites, Compos. Sci. Technol. 121 (2015) 56-72.

[47] Z. Chai, Y. Liu, et al., Reducing adhesion force by means of atomic layer deposition of ZnO films with nanoscale surface roughness, ACS Appl. Mater. Inter. 6(5) (2014) 3325-3330.

[48] W. Zhang, J. Duchet, et al., Self-healable interfaces based on thermo-reversible Diels‐Alder reactions in carbon fiber reinforced composites, J. Colloid Interf. Sci. 430 (2014) 61-68.

Declaration of interests

☑ The authors declare that they have no known competing financial interests or personal relationships that could have appeared to influence the work reported in this paper.

☐The authors declare the following financial interests/personal relationships which may be considered as potential competing interests: